Published in final edited form as:
Ann Neurol. 2011 April ; 69(4): 721–734. doi:10.1002/ana.22339.

IL-2/IL-2 Ab Therapy Induces Target Organ NK Cells that Inhibit CNS Inflammation

Junwei Hao, MD[1,2,3], **Denise Campagnolo, MD**[4,5], **Ruolan Liu, PhD**[2], **Wenhua Piao, PhD**[2], **Samuel Shi**[1,2], **Baoyong Hu, PhD**[1], **Rong Xiang, PhD**[3], **Qinghua Zhou, MD**[1], **Timothy Vollmer, MD**[6], **Luc Van Kaer, PhD**[7], **Antonio La Cava, MD, PhD**[8], and **Fu-Dong Shi, MD, PhD**[1,2]

[1] Department of Neurology, Tianjin Neurological Institute, Tianjin Medical University General Hospital, Tianjin 300052, China

[2] Department of Neurology, Barrow Neurological Institute, St. Joseph's Hospital and Medical Center, Phoenix, AZ 85013, USA

[3] School of Medicine, Nankai University, Tianjin 300071, China

[4] Neurology, Biogen Idec Inc, Cambridge, MA

[5] Department of Neurology, University of Arizona College of Medicine, Phoenix, AZ

[6] Department of Neurology, University of Colorado Denver School of Medicine, Aurora, CO 80045, USA

[7] Department of Microbiology and Immunology, Vanderbilt University School of Medicine, Nashville, TN 37232

[8] Department of Medicine, University of California, Los Angeles, CA 90095, USA

Abstract

Objective—The role of natural killer (NK) cells in regulating multiple sclerosis (MS) is not well understood. Additional studies with NK cells might provide insight into the mechanism of action of MS therapies such as daclizumab, an antibody against the IL-2R α-chain, which induces expansion of $CD56^{bright}$ NK cells.

Methods—In a relapsing-remitting form of the experimental autoimmune encephalomyelitis (EAE) model of MS induced in SJL mice, we expanded NK cells with IL-2 coupled with an anti-IL-2 mAb and evaluated the effects of these NK cells on EAE. Further, we investigated the effect of the human version of IL-2/IL-2 mAb on NK cells from MS patients and its effect on CNS inflammation and pathology in a human-mouse chimera model and assessed the underlying mechanisms.

Results—IL-2/IL-2 mAb dramatically expands NK cells both in the peripheral lymphoid organs and in the central nervous system (CNS), and attenuates CNS inflammation and neurological deficits. Disease protection is conferred by CNS-resident NK cells. Importantly, the human version of IL-2/IL-2 mAb restored the defective $CD56^{+}$ NK cells from MS patients in a human-

Corresponding author: Fu-Dong Shi, address: 350 W. Thomas Road, Phoenix, AZ 85013, phone and fax: 602-406-4094 and 602-406-8765, fshi@chw.edu.

Potential Conflicts of Interest

D. Campagnolo is an employee and stock holder of Biogen Idec. Inc. T. Vollmer received research grants and honoraria from Biogen Idec. Inc. and was involved in clinical trials of daclizumab.

mouse chimera model. Both the CD56^{bright} and CD56^{dim} subpopulations were required to attenuate disease in this model.

Interpretation—These findings unveil the immunotherapeutic potential of NK cells, which can act as critical suppressor cells in target organs of autoimmunity. These results also have implications to better understand the mechanism of action of daclizumab in MS.

Natural killer (NK) cells are large, granular lymphocytes that represent an important component of the innate immune system and operate through cytolytic activity and cytokine secretion. Both NK cell cytolytic activity and cytokine secretion have been exploited for immunotherapy of cancer and, more recently, autoimmune diseases [1–5]. Long-term, low-dose infusion of IL-2 results in selective expansion of the CD56^{bright} NK cell subpopulation [6]. Surprisingly, IL-2R blockade *in vivo* also expands the same NK cell population [1, 3, 6]. Based on these findings, the humanized anti-IL-2R α-chain mAb daclizumab has been developed and subsequently employed for treatment of autoimmune diseases, including MS and autoimmune uveitis[1, 3–5] The beneficial clinical effects of daclizumab in these diseases have been attributed, at least in part, to its capacity to expand CD56^{bright} NK cells [2, 7], which are believed to exhibit immunoregulatory functions [8].

The use of daclizumab therapy has provoked interest in further exploring the benefits of NK cell-based therapies in human organ-specific inflammatory and autoimmune diseases. This approach has also elicited several questions that are critical for understanding the role of NK cells in autoimmune diseases. First, to what extent do NK cells contribute to the protective effects of daclizumab against autoimmunity? Since lymphocytes that bear IL-2 receptors and have potential suppressive functions, such as NKT cells, CD8$^+$ T cells and CD4$^+$CD25$^+$ regulatory T cells, might also be altered by IL-2 or anti-IL-2 mAb based therapies. Second, in which anatomical compartments do NK cells demonstrate their immunosuppressive activities? Because daclizumab likely affects NK cells in all organ systems, its beneficial effects on autoimmunity might be due to events that occur in the periphery, in target organs (brain, spinal cord, or eye), or both. Third, daclizumab is only partially effective in reducing disease activity in MS. If disease attenuation is indeed linked to NK cells, will agents that have higher efficacy in inducing NK cells further improve the clinical outcome? Last, what is (are) the mechanism(s) underlying NK cell-mediated suppression of CNS pathology?

To address these questions, we first studied here the experimental autoimmune encephalomyelitis (EAE) model of relapsing-remitting MS. We compared the efficacy of IL-2, anti-IL-2 mAb and IL-2/anti-IL-2 mAb complexes in expanding NK cells in relation to the clinical manifestations of EAE, and we defined the anatomical site of action. To translate our findings to the clinical situation, we investigated the effects of the human version of IL-2 and anti-IL-2 mAb on subsets of human NK cells and to modulate disease expression in a human-mouse chimera model.

Materials and Methods

Human subjects

Collection of human blood was conducted using the protocol BNI-005: MS and Healthy Subject Tissue Acquisition for Immunological Studies, which was approved by the institutional review board. The inclusion criteria were as follows: males and females between 18 and 55 years of age with clinical definite MS as determined by McDonald criteria with a relapsing disease course and EDSS score between 0.5–6.5. Patients must have had active disease, as indicated by at least 1, but not more than 15, Gd-enhancing lesions on a screening brain 1.5T MRI. A treatment-free period of three months was employed for patients receiving immunomodulatory therapies prior to blood draw. Healthy subjects were

recruited with best effort to match with MS patients for age, gender and demography. PLP-reactive T cell lines were raised according to standard procedures [9]. Cell transfers and evaluation of disease in recipient animals are described in the Supplementary Methods.

Mice

SJL/J (H-2s) mice were purchased from The Jackson Laboratory (Bar Harbor, ME, USA). $Cx3cr1^{GFP/GFP}$ ($Cx3cr1^{-/-}$) [10] and $CD1d^{-/-}$ [11] mice were backcrossed to the SJL/J background for 8–11 generations. $RAG1^{-/-}\gamma c^{-/-}$ mice were used on a B6 background. All mice were housed in animal facilities of the Barrow Neurological Institute (Phoenix, AZ) or the Tianjin Neurological Institute (Tianjin, China).

Relapsing-remitting EAE model

The murine $PLP_{139–151}$ peptide (H-S-L-G-K-W-L-G-H-P-D-K-F) was synthesized by Biosynthesis International Co. (Lewisville, TX, USA). To induce EAE, SJL J (H-2s) mice were injected subcutaneously in the hind flank with 100 μg of $PLP_{139–151}$ peptide in complete Freund's adjuvant (CFA) (Difco, Detroit, MI, USA) containing 500 μg of heat-killed *Mycobacterium tuberculosis*, supplemented by a tail base i.v. injection of 200 ng pertussis toxin (List Biologic, Campbell, CA, USA) on day 0 and day 2. The mice were observed daily for clinical signs of disease and scored on an arbitrary scale of 0–5, with gradations of 0.5 for intermediate scores.

Antibodies and cytokines

mAbs directed against mouse NK1.1 (PK136 clone) [10], IL-2 (S4B6 clone), CD25 (PC61), and CD8 (53–6.7) were produced from hybridomas (American Type Culture Collection, Manassas, VA) and anti-mouse IFN-γ (R4-6A2) was purchased from BD Biosciences (San Diego, CA, USA). Mouse IgG2a (Sigma, St. Louis, MO) was used as an isotype control antibody. Anti-human CD25 Ab Daclizumab was provided by Biogen Idec. Anti-human IL-2 mAb was produced from DMS-1 hybridoma cells [12]. Anti-human IL-2 Rβ mAb was purchased from R&D System, Inc. Carrier-free recombinant mouse and human IL-2 was purchased from eBioscience (San Diego, CA).

For depletion of $NK1.1^+$ cells or $CD25^+$ cells in vivo, 100 μg anti-NK1.1 mAb or anti-CD25 mAb was injected i.p. into each mouse at day - 2 post immunization (p.i.). Every five days thereafter, 50 μg anti-NK1.1 mAb or anti-CD25 was injected i.p. until termination of experiments [13]. Depletion of $NK1.1^+$ and $CD25^+$ cells was confirmed by flow cytometry and was always >90%.

For preparation and administration of IL-2 and anti-IL-2 mAb complexes (referred to as IL-2 complexes hereafter), equal volumes of 30 μg/ml rIL-2 and 1 mg/ml anti-mouse IL-2 mAb in PBS were mixed in vitro and 100μl of this solution was injected i.p. into each mouse, resulting in IL-2 complexes formed by 1.5 μg of rIL-2 with 50 μg of anti-IL-2 mAb per mouse. As controls, animals were treated with rIL-2 or anti-IL-2 mAb only, and received 100μl of PBS with the same amount of either rIL-2 or anti-IL-2 mAb as for the IL-2 complexes. Additional control mice received equivalent doses of purified normal rat isotype IgG2a. Injections were repeated two times every week starting on the same day of $PLP_{139–151}$ immunization (day 0) or day 10 after immunization until termination of the experiment.

Neuropathology and neuroimaging

Mice were anesthetized with pentobarbital and perfused by intracardiac puncture with 50 ml of cold PBS. Brains and spinal cords were removed, frozen immediately and then stored at

−80°C. For evaluation of inflammatory cell infiltrates, 15-μm serial cryosections were prepared.

For imaging of reactive oxygen species (ROS) generation in brain, bioluminescence images in live mice were captured using the Xenogen IVIS200 imager (Caliper Life Sciences, Hopkinton, MA) at several time points after injection of 27 mg/kg dihydroethidium (DHE, Molecular Probes, Eugene, OR). A region of interest (ROI) tool was used to measure the fluorescent intensity. Data was collected as photons/sec/cm^2 using the Living Image® software (Caliper Life Sciences, Hopkinton, MA).

MRI was performed using a 7T small animal, 30-cm horizontal-bore magnet and BioSpec Avance III spectrometer (Bruker, Billerica, MA) with a 116 mm high power gradient set (600 mT/m) and a 72 mm whole-body mouse transmit/surface receive coil configuration. Axial and coronal T1-weighted (MSME; TE 10.5 ms, TR 322 ms, 0.5 mm slice thickness, matrix 256×256, field of view (FOV) 2.8 cm, eight averages, 40 coronal slices, scan time 22 minutes, and 20 axial slices, scan time 16 min) and fat-suppressed turbo spin echo T2-weighted (RARE; TE1 14.5 ms, TE2 65.5 ms, TR 4500 ms, 0.5 mm slice thickness, Matrix 256×256, FOV 2.8cm, eight averages, 40 coronal slices, scan time 28 minutes, and 20 axial slices, scan time 28 minutes) images were acquired, covering the volume of brain from the olfactory bulb/frontal lobe fissure to the cervical spinal cord. MRI data were analyzed using the MED×3.4.3 software package (Medical Numerics, Virginia, USA) on a LINUX workstation.

Isolation of mononuclear cells from the CNS

For CNS-infiltrating mononuclear cell isolation, at day 10–25 after EAE induction, mice were sacrificed and perfused with PBS delivered transcardially to eliminate contaminating blood cells in the CNS. Fresh brain and/or spinal cords were removed from five to six mice, cut into small pieces, and digested in 10 mM Hepes/NaOH buffer containing 1 mg/ml of collagenase for 1 hr at 37°C. Tissues were homogenized with a syringe, filtered through a 70 μM cell strainer to obtain a single cell suspension, and centrifuged. Cell pellets were resuspended in 30% percoll and centrifuged against 70% percoll. The cell monolayer between the 30%–70% percoll interface was collected as the CNS mononuclear cells for staining. Isolation of microglia from $Cx3cr1^{GFP/GFP}$ mice [14, 15] is detailed in Supplementary Figure 1.

NK cell cytotoxicity

NK cell cytotoxicity *ex vivo* was assessed by the chromium release assay using ^{51}Cr-labeled K562 human leukemia cells, as reported elsewhere [16]. Freshly purified NK cells were incubated with ^{51}Cr-labeled target cells (5×10^3) at effector cell/target cell ratio 25/1. After 4 hours of incubation, the supernatants were harvested, and ^{51}Cr-release was measured with a γ-counter (PerkinElmer, Waltham, MA). The percentage of specific lysis was calculated according to the following formula: (experimental release spontaneous release)/(maximum release –spontaneous release) × 100.

NK cell cytotoxicity toward microglia *in vivo* was assessed by the rapid elimination assay [17]. Microglia were incubated for 1 h in the presence of $Na_2{}^{51}CrO_4$ and then washed thoroughly in PBS. Groups of four to six mice were separately injected with 5×10^5 NK cells ($CD3^-CD56^+$ or $CD3^-CD56^{dim}$ or $CD3^-CD56^{bright}$) and 2×10^4 microglia in 200 μl of PBS into the brain of $RAG1^{-/-}$ $\gamma c^{-/-}$ mice as described previously [16]. The brain was removed after 8 h and the radioactivity in the brain was measured by a gamma radiation counter. The percentage of remaining radioactivity was calculated as follows: (CPM organ - CPM background)/(CPM of cells injected - CPM background) × 100.

Cell proliferation (CFSE and BrdU) assays

For carboxyfluorescein succinimidyl ester (CFSE) labeling assays, single cell suspensions (4×10^7 cells) were prepared and labeled with 0.5 μM CFSE at 37°C for 10 min. Subsequently, when cells were cultured, levels of CFSE staining declined with each cell division, allowing for cell proliferation to be monitored. Cells labeled with or without CFSE were incubated at 37°C for 3 days in round-bottomed plates (2×10^6 cells/well) with or without antigens ($PLP_{139–151}$, 10 μg/ml). After harvesting, cells were stained for surface markers with fluorochrome-conjugated mAb, including anti-CD3-PE/Cy5 (17A2), anti-CD4-allophycocyanin/Cy7 (GK1.5), and anti-CD8α-PE/Cy7 (53–6.7) (BD Biosciences). Isotype-matched mAb were used as controls.

For in vivo bromodeoxyuridine (BrdU) incorporation assays, mice were injected with 1.0 mg of BrdU (BD Biosciences) solution. After 18–24 hours, single cell suspensions were prepared from spleens and surface stained with PE-Cy7-labeled anti-CD4 (GK1.4), APC-labeled anti-CD25 (7D4) and FITC-labeled anti-BrdU mAb (3D4) according to the manufacturer's instructions (BD Biosciences). Samples were analyzed on a FACSAria™ flow cytometer (Becton Dickinson, Mountain View, CA) using Diva™ software.

FACS analysis

Single cell suspensions (10^6 cells) were prepared from spleen, lymph nodes or CNS and stained with fluorochrome-conjugated antibodies. All antibodies were purchased from BD Biosciences or eBioscience unless otherwise indicated. Antibodies were directly labeled with one of the following fluorescent tags: FITC, PE, PerCP, allophycocyanin (APC), PC5, or PC7. The following anti-mouse antibodies were employed: CD3 (145-2C11), CD4 (GK1.4), CD8 (53–6.7), CD11b (M1/70), CD11c (HL3), CD25 (7D4), NKG2A (20d5), NKG2D (CX5), Ly49D (4E5), CD244 (2B4), Ly49A (YE 1/48), Ly49C (14B11), NK1.1 (PK136), and Foxp3 (NRRF-30). Anti-human antibodies: CD3 (UCHT1), CD4 (L200), CD8 (RPA-T8), CD25 (M-A251), CD56 (B159), CD57 (NK-1), CD16 (3G8), NKG2D (1D11), NKG2A (Z199), CD94 (HP-3D9), NKp30 (p30-15), CCR7 (3D12), CD117 (YB5.B8), IL-18R (H44), CX3CR1 (2A9-1). Flow cytometric data were collected on a FACSAria™ flow cytometer (Becton Dickinson, Mountain View, MD) and analyzed with Diva™ software. Isotype-matched negative control mAbs were used for all stains. To determine the percentage of cells producing selected cytokines, values obtained with isotype controls were subtracted from those with specific mAb.

Cytokines, perforin and granzyme B quantification

For intracellular cytokine staining, single cell suspensions were prepared and incubated at 37°C for four days in round-bottomed plates (2×10^6 cells/well) with or without antigens ($PLP_{139–151}$,10 μg/ml or Con A, 5 μg/ml), and stimulated with a mixture of PMA (20 ng/ml), ionomycin (1 μg/ml), and brefeldin A (5 μg/ml) for another 5 h at 37°C. After harvesting, cells were stained for surface markers, fixed and permeabilized with Cytofix/Cytoperm kit (BD Biosciences), then stained with anti-IFN-γ mAb (XMG1.2), and anti-IL-17 mAb (TC11-18H10) conjugated with Alexa 647 or PE. For intracellular Foxp3 expression, fresh cells were stained for surface markers with anti-CD4-FITC (H129.19) and anti-CD25-allophycocyanin (PC61.5) for 15 min at 4°C, fixed, permeabilized, and then stained with anti-Foxp3-PE (FJK-16s) (eBioscience, San Diego, CA). All samples were analyzed on a FACSAria™ using Diva™ software.

ELISA using BD optEIA kits or eBioscience kits was performed for assessment of cytokine release by IL-2 complex-expanded mouse and human NK cells (IFN-γ and MIP1α). Perforin and granzyme B were quantified by ELISA according to the manufacturer's instructions (Abcam, Cambridge, UK).

qRT-PCR

Total RNA was extracted from cell suspensions of spinal cords using TRIzol (Invitrogen Life Technologies, Carlsbad, CA). First strand cDNA of each sample was synthesized using a reverse transcription kit (Invitrogen, Carlsbad, CA). RT-PCR was performed as previously described, using an ABI Prism 7900-HT sequence system (PE Applied Biosystems) with the QuantiTect SYBR Green PCR kit (Qiagen), in accordance with the manufacturer's instructions. The following primers were used: Foxp3 F: 5′-CCCAGGAAAGACAGCAACCTT-3′, R: 5′-CCCAGGAAAGACAGCAACCTT-3′; HPRT F: 5′-AGC CTA AGA TGA GCG CAA GT-3′, R: 5′-TTA CTA GGC AGA TGG CCA CA-3′; IL-17 F: 5′-ATGACTCCTGGGAAGACCTCATTG-3′, R: 5′-TTAGGCCACATGGTGGACAATCGGTTA′; Rorc F: 5′-AGTCGGAAGGCAAGATCAGA-3′, R: 5′-CAAGAGAGGTTCTGGGCAAG-3′; β-actin F: 5′-GGACTTCGAGCAAGAGATGG-3′, R: 5′-TGTGTTGGCGTACAGGTCTTTG-3′. The hypoxanthine-guanine phosphoribosyl transferase (HPRT) or β-actin gene was amplified and served as an endogenous control. 1 μl of first strand cDNA product was amplified with platinum Taq polymerase (Invitrogen) and gene-specific primer pairs. Each sample was assayed in triplicate and experiments were repeated twice. The relative amounts of mRNA were calculated by plotting the Ct (cycle number), and average relative expression was determined by the $2^{-\Delta\Delta Ct}$ comparative method.

RESULTS

IL-2/anti-IL-2 mAb complexes expand NK cells in the periphery and in the CNS

To expand NK cells in vivo, we coupled IL-2 with the IL-2 neutralizing antibody S4B6. The S4B6 mAb stimulates the proliferation of NK cells and, to some degree, memory $CD8^+$ T cells[18]. After induction of EAE, mice were treated with IgG, IL-2, anti-IL-2, or IL-2/anti-IL-2 mAb complexes two times every week until termination of the experiments. This protocol of injection with IL-2 complexes - determined by comparing different treatment frequencies, durations and dosages (Supplementary Table 1 and data not shown) - expanded NK cells about 3- to 5-fold in the spleen, lymph nodes and blood (Fig 1A, and data not shown). Similarly, the percentages of CNS-resident NK cells in mice receiving IL-2 complexes were also expanded 3- to 5-fold (Fig 1A).

Phenotypically, expanded NK cells expressed similar levels of the activating receptor NKG2D compared with NK cells from control mice (Fig 1B), whereas the inhibitory receptor NKG2A was significantly upregulated (Fig 1C). The expression of several other activating or inhibitory receptors, including Ly49D, CD244, Ly49A, and Ly49C were not significantly altered (data not shown). Additionally, expanded NK cells produced more IFN-γ and MIP1α than controls (Fig 1D).

Concomitantly, IL-2 complexes reduced the numbers of $CD4^+$ T cells and increased $CD8^+$ T cells with a memory phenotype (Supplementary Fig 2A and B). $CD4^+CD25^+Foxp3^+$ Treg and NKT cells were marginally increased (not significant) (Supplementary Fig 2C, and data not shown). These cellular changes in the mice receiving IL-2 complexes remained relatively constant throughout the experiment (Supplementary Table 1).

IL-2 complexes attenuate disease activity and CNS pathology

We assessed the capacity of IL-2 complex injection to modulate disease activity and the magnitude of inflammatory and autoimmune responses in the CNS. Compared to control animals, mice receiving IL-2 complexes during disease induction experienced delayed disease onset, a prolonged interval between relapses, and reduced disease severity (Fig 2A and Supplementary Table 2). Consistent with these findings, treated mice had milder

inflammation, demyelination and more axonal integrity, as measured by immunohistochemical staining, bio-fluorescent imaging and high-field MRI imaging, respectively (Fig 2B–D). Notably, IL-2 complex administration at the initial peak stage of disease, or during remission, also attenuated severity of disease, although the efficacy was less impressive than treatment during disease induction (Fig 2A; Supplementary Tables 2 and 3). Collectively, these data indicate the superior effectiveness of IL-2 complexes in ameliorating clinical EAE and CNS pathology.

IL-2 complexes differentially modulate myelin-reactive Th17 cells in lymph nodes and CNS

Occurrence of the clinical neurological deficits presented by mice with EAE and perhaps in patients with MS requires entry of myelin-reactive T cells, particularly $CD4^+$ T cells, into the CNS [19], followed by reactivation and further differentiation of these cells within this compartment. Therefore, we compared the capacity of PLP-reactive $CD4^+$ T cells to proliferate in control mice and in mice that received IL-2 complexes. For lymph node cells from mice that received IL-2 complexes, we observed a 2- to 3-fold reduction in PLP-induced proliferation. Such reduced proliferation was more evident (3- to 4-fold) in the CNS (Fig 3A). Next, we assessed PLP-reactive Th1 and Th17 cell responses, the two The cell subsets that have been implicated in orchestrating CNS destruction [20–22]. A marginal (not statistically significant) reduction in the frequency of PLP-reactive, Th17 cells was observed in the lymph nodes of mice that received IL-2 complexes, but such responses were significantly reduced in the CNS (Fig 3B). For IFN-γ producing $CD4^+$ T cells, we observed a moderate reduction in both the periphery and CNS (Fig 3B). IFN-γ and IL-17A transcripts were affected similarly by IL-2 complexes in both compartments (data not shown). The effects of IL-2 complexes on autoreactive $CD8^+$ T cells were similar to those on $CD4^+$ T cells, although expression of IL-17 in $CD8^+$ cells was minimal (data not shown). Thus, IL-2 complexes preferentially silence myelin-reactive Th17 cells and, to a lesser extent, Th1 cells in the CNS. Further investigation revealed that this is less likely due to the altered migratory capacity of Th1 and Th17 cells, as expression of the chemokine receptor CCR5 and the integrins VLA-4 and LFA-1 was not influenced by IL-2 complexes (data not shown).

The effects of IL-2 complexes on EAE are dependent on CNS-resident NK cells

We used two complementary approaches to dissect the involvement of NK cells in different anatomical compartments during IL-2 complex therapy. The first approach used an anti-NK1.1 mAb (PK136), which eliminates NK cells in all organs (including the CNS) during EAE [23], an event that is associated with exacerbated EAE in both B6 and SJL mice [23]. We confirmed disease exacerbation after NK cell depletion (Fig 4A), and found that IL-2 complexes in animals depleted of NK cells did not alter the course of EAE, indicating that IL-2 complexes require NK cells to exert their therapeutic effects (Fig 4A).

To distinguish between the contribution of peripheral vs. CNS-resident NK cells in IL-2 complex therapy, we cross-bred SJL mice with $Cx3cr1^{GFP/GFP}$ mice. The chemokine receptor CX3CR1 is expressed by monocytes, DCs, subsets of T cells, and NK cells in the circulation, and is expressed in the CNS exclusively on microglia [15, 24–28]. The only ligand for CX3CR1 is fractalkine (CX3CL1) [24, 28], which has been shown to recruit NK cells to the inflamed CNS in mice with EAE [10, 29, 30]. NK cells were enriched in the peripheral lymphoid organs of PLP-immunized $Cx3cr1^{-/-}$ mice (Fig 4B, and data not shown) but they were significantly reduced in the CNS, irrespective of IL-2 complex treatment (Fig 4B). Consistent with our previous findings in the C57BL/6 model [15], PLP-primed $Cx3cr1^{-/-}$ exhibited more severe clinical and pathological EAE than wild type mice (Fig 4C, and data now shown). Thus, lack of CNS-resident NK cells, even with intact NK cells in the periphery, leads to exacerbated disease, which underscores the importance of the suppressive effect of NK cells within the CNS.

Interestingly, EAE in IL-2 complex-treated Cx3cr1$^{-/-}$ mice was indistinguishable for disease onset, severity and relapses from Cx3cr1$^{-/-}$ mice receiving control IgG (Fig 4C). Thus, the efficacy of IL-2 complexes in this model depends on CNS-resident NK cells.

NKT cells, Treg cells and CD8$^+$ T cells in disease protection induced by IL-2 complexes

To study NKT cells during IL-2 complex therapy, we cross-bred SJL mice with CD1d$^{-/-}$ mice (lacking CD1d-restricted NKT cells) [11]. CD1d$^{-/-}$ mice receiving IL-2 complexes exhibited EAE with milder severity and fewer relapses, compared with CD1d$^{-/-}$ mice that received IgG (Supplementary Table 4). Similarly, IL-2 complexes were equally effective in control mice compared with mice receiving anti-CD8 mAb prior to EAE induction (Supplementary Table 4). To investigate a possible role for Treg cells, anti-CD25 depleting mAb (PC61) was injected prior to EAE induction [13]. Anti-CD25 mAb exacerbated EAE, with a gradual increase in the rate of relapses and disease severity, and injection of IL-2 complexes in CD25$^+$ cell-depleted mice resulted in reduced EAE severity. The overall clinical parameters in this group of mice were indistinguishable from that of control mice (Fig 4D).

Collectively, these results suggest that the protective effects of IL-2 complexes are due to NK cells and less likely to CD8$^+$ T cells, NKT cells or CD4$^+$CD25$^+$ T cells.

Human IL-2 complexes restore defective NK cells from MS patients

Having determined the efficacy and mechanisms of action of IL-2 complexes against EAE in SJL mice, we sought to translate these findings to patients with relapsing-remitting MS. For this purpose, we compared the effect of human IL-2, anti-human IL-2 mAb, daclizumab, anti-human IL-2Rβ mAb, and a combination of IL-2 and anti-IL-2 mAb (IL-2 complexes) on NK cells from healthy subjects and treatment-naïve, relapsing-remitting MS patients (Supplementary Table 5). Consistent with previous reports [31], the numbers of CD3$^-$CD56$^+$, CD57$^+$ NK cells in MS patients were reduced and their cytotoxicity toward K562 target cells was compromised (Fig 5B), as compared with healthy controls. We focused on CD3$^-$CD56$^+$ NK cells because this population has been suggested to contribute to protective effects in patients treated with daclizumab [1–3]. CD56-expressing NK cells are classified as cytokine-producing (CD56^{brigh}) and cytotoxic (CD56^{dim}) NK cell subsets. We demonstrated that IL-2 complexes strongly enhanced production of IFN-γ and MIP-1α by sorted CD56^{bright} cells (Fig 5C) and increased the efficacy of K562 target cell killing by sorted CD56^{dim} cells (Fig 5B), to an extent similar to or surpassing NK cells from normal subjects. The increased cytotoxicity was associated with increased perforin, and to a lesser extent, granzyme B secretion (Fig 5D).

In addition, expression of NKG2A was slightly upregulated by IL-2 complexes, whereas expression of NKG2D and NKp30 was not significantly altered by IL-2 complex treatment (Fig 5A and data not shown). Expression of CD94 was also upregulated (Fig 5E). Compared to IL-2 or anti-IL-2 mAb, IL-2 complexes exhibited greater efficacy in restoring and/or expanding CD56$^+$ NK cells than IL-2 or anti-IL-2 mAb alone in both MS patients and controls (Fig 5A, C and Supplementary Table 5). Effects of IL-2 complexes on Treg cells, NKT cells, CD8$^+$ cells and CD4$^+$ cells were varied and differences among the groups did not reach statistical significance (Supplementary Table 5).

Both CD56^{bright} and CD56^{dim} NK cells are required to attenuate EAE severity

CD56^{bright} cells have been suggested to be the relevant “regulatory cells” that contribute to reduction of the myelin-reactive T cell compartment and disease activity in MS and uveitis patients treated with daclizumab [1–3]. Direct evidence in support of this notion is lacking. Therefore, we created a human-mouse chimera model and directly tested whether adoptive

transfer of $CD56^+$ cells and their subsets can modulate EAE in $RAG1^{-/-}\gamma c^{-/-}$ mice induced by a PLP-reactive human T cell line. This T cell line was raised [9] from the same donors for phenotyping studies. Prior to NK cell transfer, $CD56^{bright}$ and $CD56^{dim}$ NK cell subsets were further verified by differential expression of CCR7, CD117, IL-18R, and CX3CR1 (Fig 6A). CD16 was also incorporated as an aid to separate $CD56^{dim}$ and $CD56^{bright}$ populations in some subjects [32]. Our results indicated that transfer of $CD56^{bright}$ cells pre-treated with IL-2 complexes had a tendency to ameliorate EAE severity (Fig 6A). Surprisingly, transfer of $CD56^{dim}$ NK cells also ameliorated disease (Fig 6A). Interestingly, the most impressive disease protection was achieved by transfer of total $CD56^+$ cells containing both bright and dim populations (Fig 6A). Transfer of $CD56^+$ NK cells and its subsets without exposure to IL-2 complexes produced minimum clinical benefits (data not shown). IL-2 complexes boosted the capacity of total $CD56^+$ NK cells and the two subsets of $CD56^+$ NK cells to proliferate in recipient mice (Fig. 6B). Therefore, both subpopulations are required to modulate the magnitude of inflammatory and autoimmune responses in the CNS.

Human NK cells employ two means for disease protection: cytotoxicity and cytokine production

Requirement of both $CD56^{bright}$ and $CD56^{dim}$ subpopulations of NK cells suggests that diverse mechanisms might be utilized by the transferred NK cells in recipient mice. A recent study using a C57BL/6 model of EAE suggested that microglia are very potent in driving myelin-reactive Th17 cells when the suppressive effect of NK cells in situ is absent, and that this suppression was achieved by breaking NK cell tolerance due to loss of the self MHC class Ib molecule Qa1 on activated microglia [16]. Our results in the SJL model also support this finding (data not shown). Although these data provide evidence that microglia serve as a primary NK cell target during CNS inflammation in the C57BL/6 and SJL models of EAE, mouse NK cells do not express CD56 and, in contrast with human NK cells, cytotoxic and cytokine-releasing subpopulations are not distinguishable. Investigation of these aspects in a humanized model not only provides additional evidence regarding the role of NK cell and microglia cell interactions in shaping disease expression, but also leads to new insight on functions of human NK cell subsets and their relevance in pathology and immune therapy. For these purposes, we co-transferred NK cells, microglia and T cells into recipient $RAG1^{-/-}\gamma c^{-/-}$ mice. A rapid elimination assay revealed that $CD56^{dim}$ cells can lyse microglia in vivo (Fig. 7A, B). Both $CD56^{dim}$ and $CD56^{bright}$ subsets reduced the capacity of microglia to transactivate the Th17 transcription factor Rorc, blunted Th17 responses (Fig. 7C, D) and attenuated EAE (data not shown). For $CD56^{bright}$ NK cells, neutralization of IFN-γ reversed these effects to a large degree (Figure 7D). Transfer of $CD56^+$ NK cells and its subsets without exposure to IL-2 complexes exerted only a marginal impact on Th17 cells and produced minimal clinical benefits (data not shown). Therefore, these data extend the C57BL/6 study substantially and suggest that cytotoxicity and cytokine production are two effector mechanisms employed by NK cells for disease suppression, and both APCs and T cells [33] (Supplementary Fig. 3) may become targets for NK cell.

Discussion

It has long been recognized that NK cells are present with reduced numbers and compromised functions in many human autoimmune diseases, including MS [34]. Such phenotypes of NK cells in autoimmune diseases resemble those of other regulatory cells such as Treg cells and NKT cells [35]. Although the defective NK cells and other regulatory cells found in autoimmune diseases could be a secondary phenomenon to the aberrant autoimmune responses, it could lead to occurrence and/or progression of autoimmunity. If functional NK cell deficiency is indeed linked to the progression of autoimmunity, the

question arises whether restoration of the defective NK cells can improve the clinical outcome in patients. The promising results from daclizumab, a humanized anti-IL-2R α-chain mAb, in MS and uveitis support this intriguing hypothesis. If expansion of so-called "regulatory NK cells" found in patients with MS and uveitis is indeed responsible for the improved clinical picture in these patients, then, a more efficient way of inducing NK cells would be expected to confer improved protection against autoimmunity and may re-establish long-term tolerance to autoantigens in patients with autoimmune diseases.

The common γ-chain (γc) cytokines IL-2 and IL-15 have been identified as NK cell growth factors. Understanding the biology of these cytokines is critical to optimize NK cell-based therapies in autoimmune disorders and cancer. The receptor for IL-2 is formed by three chains (α, β and γ_c). A high-affinity receptor of IL-2 is composed of all three chains (IL-2Rα$\beta\gamma_c$): the α-chain (CD25), the β-chain (CD122) and the common γ-chain (γ_c). The IL-2R$\beta\gamma_c$ heterodimer has intermediate affinity for IL-2. Daclizumab is a humanized mAb that targets the α-chain of the high affinity receptor. The exact means by which daclizumab expands NK cells is not clear, although a recent study suggested that daclizumab blocks IL-2 signaling in T cells and increases the availability of IL-2 to NK cells and, therefore, expanding NK cells [36]. An alternative means to increase the bio-availability of IL-2 is to apply antibodies bound to a cytokine, which can lead to paradoxically enhanced immune effects than cytokine treatment only, likely due to prolongation of cytokine bioactivity [37]. This approach also lowers the therapeutic doses of cytokines and thereby reduces adverse side-effects [38].

Based on the experience with daclizumab and recent advances in IL-2 biology, we first compared the capacity of mouse IL-2, IL-15 and IL-2 coupled with an antibody to IL-2 (S4B5 clone with intermediate affinity) to expand NK cells and to modify disease expression in a relapsing-remitting form of neurological deficits in SJL mice. We found that IL-2 complexes are superior to IL-2 or IL-15 in expanding NK cells and attenuating EAE when administered before immunization and after the appearance of neurological deficits. Further investigations revealed that CNS-resident NK cells are largely responsible for the generation of blunted myelin-reactive Th17 cell responses, and this occurs preferentially in the CNS. A recent study provided additional evidence supporting this finding in a C57BL/6 model and further suggested that microglia can serve as principal targets of NK cells in the brain, due to activation-induced loss of self MHC class I expression [16].

Do the studies with SJL and C57BL/6 models of EAE help understand the efficacy of daclizumab therapy? This is challenging for a number of reasons. First human and mouse NK cells express different markers. Consequently, CD56, CD57 and CD16 are used to identify human NK cells, whereas NK1.1 and/or DX5 are used for mouse NK cells. Second, differential expression of CD56 marks human NK cell subsets with either cytotoxic or cytokine-producing properties, and such subsets cannot be distinguished in mouse NK cells by CD56 but likely by CD27[39]. Third, human NK cells are present at reduced numbers and exhibit decreased cytotoxicity, whereas none of these features are present in mice with EAE. Our means to expand NK cells in the mouse model does not imply the same capacity in MS patients. Lastly, the murine and human versions of IL-2 and anti-IL-2 mAb with intermediate affinity activate NK cells with different mechanisms than daclizumab, which engages the high affinity IL-2 receptor.

To address these challenges, we tested the efficacy of human IL-2 coupled with an anti-IL-2 mAb for restoration of NK cell functions from patients with relapsing-remitting MS and assessed the ability of these human NK cells, after treatment with IL-2 complexes, to modulate EAE in a humanized model. We demonstrated that IL-2 complexes are more potent than dacluzimab in expanding NK cells (Supplementary Table 5) [18]. Engagement of

the β-chain of IL-2R increases the affinity of the signaling complex for IL-2[36], which may serve as the basis for the augmented efficacy of IL-2 complexes in expanding NK cells. It is conceivable that the mechanisms of action of daclizumab and the murine and human version of IL-2 complexes are distinct, but expansion of NK cells appears to be a common correlate of treatment efficacy. Thus, these reagents mirror each other and affirm NK cells as valuable and unique targets for immune therapies in inflammatory and autoimmune conditions of the CNS. Further, since both $CD56^{bright}$ and $CD56^{dim}$ subsets of NK cells are required for disease protection, a combination of cytokines and mAbs coupled with cytokines, or engagement of IL-2R at distinct levels of strength, may prove to be more effective in expanding NK cell subsets that are specialized for cytokine production or cytotoxicity. Further, engagement of IL-2R with antibodies of high affinity was shown to expand regulatory T cells and inhibit EAE and mAb-mediated autoimmune myasthenia gravis [1, 40].

In summary, this study has identified the differential roles of NK cells, depending on their anatomical location, on CNS autoimmunity. Importantly, a scientific foundation for using IL-2 coupled with antibodies against IL-2 is established for treatment of MS and other organ-specific autoimmune diseases. In certain situations, NK cells can have a detrimental effect on disease [15, 24–28, 30], and in other situations, as demonstrated here, NK cells can inhibit inflammatory and autoimmune responses. Decisions for such contrasting effects may stem from the timing of an immune response and/or organ-specific factors. Progress in the understanding of these aspects of NK cell biology will further the development of NK cell-based therapies of inflammatory and autoimmune diseases.

Supplementary Material

Refer to Web version on PubMed Central for supplementary material.

Acknowledgments

We thank Drs. D. Huang and R. Ransohoff for collaborations on work performed with $Cx3cr1^{GFP/GFP}$ mice, S. Rhodes and D. Dayao for technical support, G. Turner for expertise on 7T MRI, and our patients for donating blood samples. This study was supported in part by the Tianjin Medical University General Hospital (F.D. Shi), Tianjin Science and Technology Commission (F.D. Shi), the Arizona Biomedical Research Commission (9-140 to F.D. Shi) and the NIH (R01AI083294 to F.D. Shi; R01AR53293 to A. La Cava; R01AI070305 and HL089667 to L. Van Kaer). J. Hao is supported by China Scholarship Council 2008622008. R. Liu is a Hobb Family Neuroimmunology Fellow.

References

1. Li Z, Lim WK, Mahesh SP, et al. Cutting edge: in vivo blockade of human IL-2 receptor induces expansion of CD56(bright) regulatory NK cells in patients with active uveitis. J Immunol. 2005; 174:5187–5191. [PubMed: 15843513]
2. Bielekova B, Howard T, Packer AN, et al. Effect of anti-CD25 antibody daclizumab in the inhibition of inflammation and stabilization of disease progression in multiple sclerosis. Archives of neurology. 2009; 66:483–489. [PubMed: 19364933]
3. Bielekova B, Catalfamo M, Reichert-Scrivner S, et al. Regulatory CD56(bright) natural killer cells mediate immunomodulatory effects of IL-2Ralpha-targeted therapy (daclizumab) in multiple sclerosis. Proc Natl Acad Sci U S A. 2006; 103:5941–5946. [PubMed: 16585503]
4. Wynn D, Kaufman M, Montalban X, et al. Daclizumab in active relapsing multiple sclerosis (CHOICE study): a phase 2, randomised, double-blind, placebo-controlled, add-on trial with interferon beta. Lancet neurology. 2010; 9:381–390. [PubMed: 20163990]
5. Rose JW, Watt HE, White AT, Carlson NG. Treatment of multiple sclerosis with an anti-interleukin-2 receptor monoclonal antibody. Annals of neurology. 2004; 56:864–867. [PubMed: 15499632]

6. Caligiuri MA, Murray C, Robertson MJ, et al. Selective modulation of human natural killer cells in vivo after prolonged infusion of low dose recombinant interleukin 2. J Clin Invest. 1993; 91:123–132. [PubMed: 7678599]
7. Rose JW, Burns JB, Bjorklund J, et al. Daclizumab phase II trial in relapsing and remitting multiple sclerosis: MRI and clinical results. Neurology. 2007; 69:785–789. [PubMed: 17709711]
8. Cooper MA, Fehniger TA, Caligiuri MA. The biology of human natural killer-cell subsets. Trends Immunol. 2001; 22:633–640. [PubMed: 11698225]
9. Teitelbaum D, Milo R, Arnon R, Sela M. Synthetic copolymer 1 inhibits human T-cell lines specific for myelin basic protein. Proceedings of the National Academy of Sciences of the United States of America. 1992; 89:137–141. [PubMed: 1370347]
10. Huang D, Shi FD, Jung S, et al. The neuronal chemokine CX3CL1/fractalkine selectively recruits NK cells that modify experimental autoimmune encephalomyelitis within the central nervous system. Faseb J. 2006; 20:896–905. [PubMed: 16675847]
11. Mendiratta SK, Martin WD, Hong S, et al. CD1d1 mutant mice are deficient in natural T cells that promptly produce IL-4. Immunity. 1997; 6:469–477. [PubMed: 9133426]
12. Smith KA, Favata MF, Oroszlan S. Production and characterization of monoclonal antibodies to human interleukin 2: strategy and tactics. J Immunol. 1983; 131:1808–1815. [PubMed: 6352804]
13. Liu R, La Cava A, Bai XF, et al. Cooperation of invariant NKT cells and CD4+CD25+ T regulatory cells in the prevention of autoimmune myasthenia. J Immunol. 2005; 175:7898–7904. [PubMed: 16339525]
14. Cardona AE, Huang D, Sasse ME, Ransohoff RM. Isolation of murine microglial cells for RNA analysis or flow cytometry. Nature protocols. 2006; 1:1947–1951.
15. Cardona AE, Pioro EP, Sasse ME, et al. Control of microglial neurotoxicity by the fractalkine receptor. Nature neuroscience. 2006; 9:917–924.
16. Hao J, Liu R, Piao W, et al. Central nervous system (CNS)-resident natural killer cells suppress Th17 responses and CNS autoimmune pathology. The Journal of experimental medicine. 2010; 207:1907–1921. [PubMed: 20696699]
17. Hayakawa Y, Screpanti V, Yagita H, et al. NK cell TRAIL eliminates immature dendritic cells in vivo and limits dendritic cell vaccination efficacy. J Immunol. 2004; 172:123–129. [PubMed: 14688317]
18. Boyman O, Kovar M, Rubinstein MP, et al. Selective stimulation of T cell subsets with antibody-cytokine immune complexes. Science. 2006; 311:1924–1927. [PubMed: 16484453]
19. Bartholomaus I, Kawakami N, Odoardi F, et al. Effector T cell interactions with meningeal vascular structures in nascent autoimmune CNS lesions. Nature. 2009; 462:94–98. [PubMed: 19829296]
20. Chung Y, Chang SH, Martinez GJ, et al. Critical regulation of early Th17 cell differentiation by interleukin-1 signaling. Immunity. 2009; 30:576–587. [PubMed: 19362022]
21. McGeachy MJ, Chen Y, Tato CM, et al. The interleukin 23 receptor is essential for the terminal differentiation of interleukin 17-producing effector T helper cells in vivo. Nat Immunol. 2009; 10:314–324. [PubMed: 19182808]
22. Komiyama Y, Nakae S, Matsuki T, et al. IL-17 plays an important role in the development of experimental autoimmune encephalomyelitis. J Immunol. 2006; 177:566–573. [PubMed: 16785554]
23. Zhang B, Yamamura T, Kondo T, et al. Regulation of experimental autoimmune encephalomyelitis by natural killer (NK) cells. The Journal of experimental medicine. 1997; 186:1677–1687. [PubMed: 9362528]
24. Biber K, Neumann H, Inoue K, Boddeke HW. Neuronal ‘On’ and ‘Off’ signals control microglia. Trends Neurosci. 2007; 30:596–602. [PubMed: 17950926]
25. Hanisch UK, Kettenmann H. Microglia: active sensor and versatile effector cells in the normal and pathologic brain. Nature neuroscience. 2007; 10:1387–1394.
26. Pan Y, Lloyd C, Zhou H, et al. Neurotactin, a membrane-anchored chemokine upregulated in brain inflammation. Nature. 1997; 387:611–617. [PubMed: 9177350]
27. Bazan JF, Bacon KB, Hardiman G, et al. A new class of membrane-bound chemokine with a CX3C motif. Nature. 1997; 385:640–644. [PubMed: 9024663]

28. Campbell JJ, Qin S, Unutmaz D, et al. Unique subpopulations of CD56+ NK and NK-T peripheral blood lymphocytes identified by chemokine receptor expression repertoire. J Immunol. 2001; 166:6477–6482. [PubMed: 11359797]
29. Jung S, Aliberti J, Graemmel P, et al. Analysis of fractalkine receptor CX(3)CR1 function by targeted deletion and green fluorescent protein reporter gene insertion. Mol Cell Biol. 2000; 20:4106–4114. [PubMed: 10805752]
30. Nimmerjahn A, Kirchhoff F, Helmchen F. Resting microglial cells are highly dynamic surveillants of brain parenchyma in vivo. Science (New York, NY). 2005; 308:1314–1318.
31. Shi FD, Van Kaer L. Reciprocal regulation between natural killer cells and autoreactive T cells. Nat Rev Immunol. 2006; 6:751–760. [PubMed: 16998508]
32. Yu J, Mao HC, Wei M, et al. CD94 surface density identifies a functional intermediary between the CD56bright and CD56dim human NK-cell subsets. Blood. 2010; 115:274–281. [PubMed: 19897577]
33. Leavenworth JW, Schellack C, Kim HJ, et al. Analysis of the cellular mechanism underlying inhibition of EAE after treatment with anti-NKG2A F(ab′)2. Proceedings of the National Academy of Sciences of the United States of America. 107:2562–2567. [PubMed: 20133787]
34. Kastrukoff LF, Morgan NG, Zecchini D, et al. Natural killer cells in relapsing-remitting MS: effect of treatment with interferon beta-1B. Neurology. 1999; 52:351–359. [PubMed: 9932956]
35. Kastrukoff LF, Morgan NG, Aziz TM, et al. Natural killer (NK) cells in chronic progressive multiple sclerosis patients treated with lymphoblastoid interferon. Journal of neuroimmunology. 1988; 20:15–23. [PubMed: 3183034]
36. Martin JF, Perry JS, Jakhete NR, et al. An IL-2 paradox: blocking CD25 on T cells induces IL-2-driven activation of CD56(bright) NK cells. J Immunol. 185:1311–1320. [PubMed: 20543101]
37. Courtney LP, Phelps JL, Karavodin LM. An anti-IL-2 antibody increases serum half-life and improves anti-tumor efficacy of human recombinant interleukin-2. Immunopharmacology. 1994; 28:223–232. [PubMed: 7852053]
38. Prlic M, Bevan MJ. Immunology. An antibody paradox, resolved. Science (New York, NY). 2006; 311:1875–1876.
39. Hayakawa Y, Huntington ND, Nutt SL, Smyth MJ. Functional subsets of mouse natural killer cells. Immunological reviews. 2006; 214:47–55. [PubMed: 17100875]
40. Webster KE, Walters S, Kohler RE, et al. In vivo expansion of T reg cells with IL-2-mAb complexes: induction of resistance to EAE and long-term acceptance of islet allografts without immunosuppression. The Journal of experimental medicine. 2009; 206:751–760. [PubMed: 19332874]

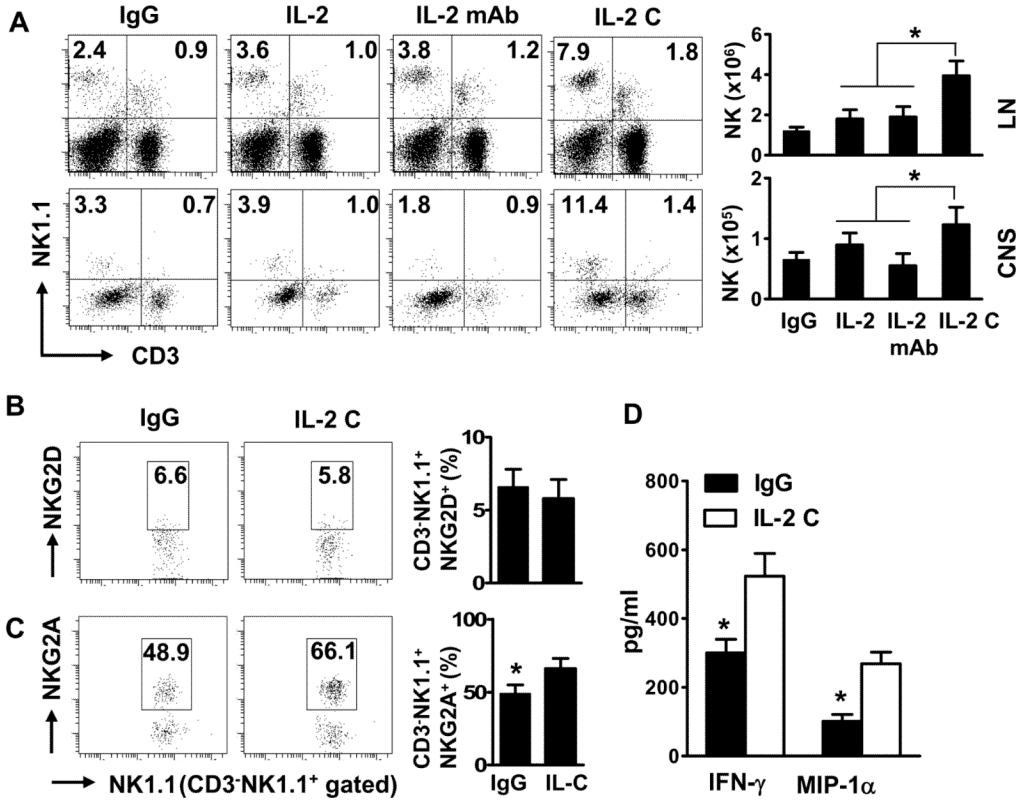

FIGURE 1. IL-2/anti-IL-2 mAb complexes expand NK cells in the periphery and the CNS

After EAE induction with PLP, SJL/J mice were treated with control IgG, IL-2, anti-IL-2 mAb (S4B6), or a combination of IL-2 and anti-IL-2 mAb (IL-2 C) i.p., on the same day of $PLP_{139–151}$ immunization until termination of the experiment, as described in detail in the *M & M*. Single cell suspensions were prepared from spleens and CNS on days 10–20 post immunization (p.i.). Frequency and phenotypes of mononuclear cells were analyzed by FACS. (A) Frequency and numbers of NK and NKT cells in the periphery and CNS on gated lymphocytes in corresponding compartments. (B, C) Expression of NKG2A and NKG2D on gated $NK1.1^{+}CD3^{-}$ cells. (D) Lymphocytes isolated from mouse LN tissues were cultured with IgG or IL-2 C for 48–72 hours. Production of IFN-γ and MCP-1α by sorted NK cells was measured by ELISA. The data of one experiment out of two performed is shown, n = 3–4 mice/group. Dot plots are representative of two separate experiments (n=6–18 mice). P values, Student's *t*-test, *p<0.05.

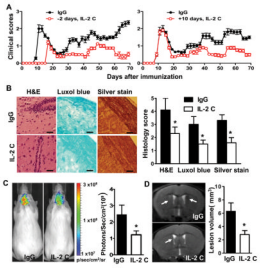

FIGURE 2. IL-2 complexes inhibit EAE activity and CNS pathology

Mice were immunized with PLP/CFA and treated with IgG or IL-2 complexes (IL-2 C) prior to or after immunization. (A) EAE scores were recorded as mean clinical scores ± SD. Left panel denotes IL-2 C administration before or during EAE induction, n= 18–20 mice/group; right panel IL-2 C administration at day 10 p.i., n=6–8 mice/group. (B) Immunohistochemical analysis of intensity of infiltration, demyelination and axonal loss of spinal cords harvested at days 10–25 p.i. Results are representative of two experiments. (C) *In vivo* bioluminescence imaging analyses of brains at days 10–25 p.i. using Xenogen IVIS spectrum. Results are expressed as the region of interest (ROI) measurements of brain by Loess regression statistical analyses. (D) Visualization of brain demyelination with 7TMRI. Arrow heads indicate focal lesions located around the lateral ventricle and increased signal intensity on T2-weighted lesions. Pathology and imaging experiments were conducted in groups of mice (n= 4) between 10–25 days post immunization. Data are representative of two independent experiments (mean and s.e.m.). Scale bar, 100 μm. P values for clinical scores were evaluated by Mann-Whitney *U* test, all other comparisons between groups were analyzed by Student's *t*-test for two groups and ANOVA for multiple comparisons; *p<0.05, **p<0.01.

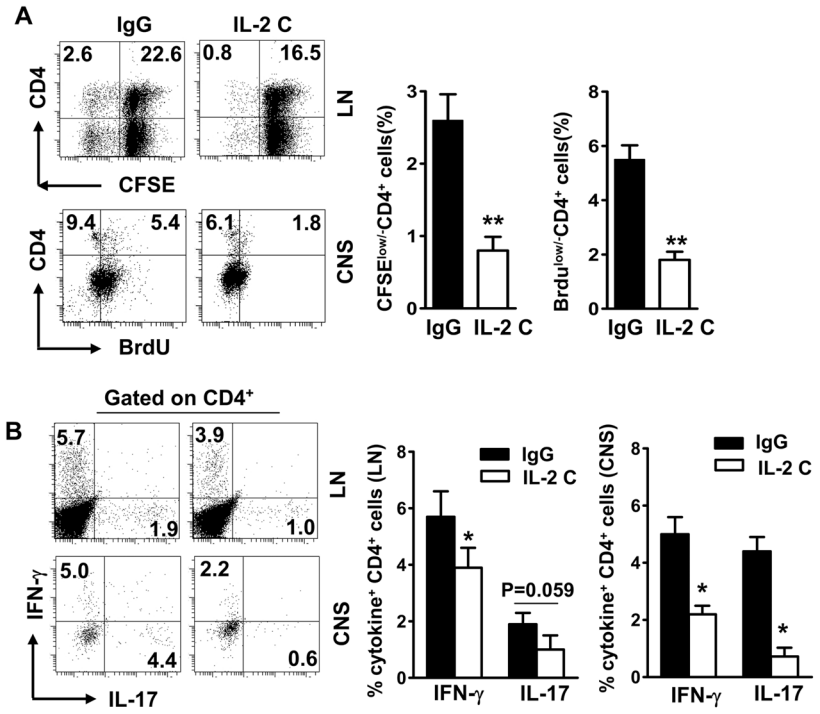

FIGURE 3. IL-2 complexes preferentially inhibit myelin-reactive Th17 cells in the CNS

Mice were primed with PLP/CFA and treated with IgG or IL-2 complexes (IL-2 C). Mice were sacrificed at day 10–25 post-immunization (p.i.). Lymph node and CNS cells were isolated. (A) Expansion of $CD4^+$ T cells in the periphery and in the CNS on gated lymphocytes was assessed by CFSE dilution or BrdU incorporation assay, respectively. (B) Lymphoid or CNS cells were re-stimulated with PLP overnight and IFN-γ- and IL-17-expressing $CD4^+$ T cells were measured by intracellular staining. FACS dot plots are representative of four independent experiments (n= 6–15/group). Bar data were accumulated from four independent experiments; P values were calculated by Student's *t*-test.

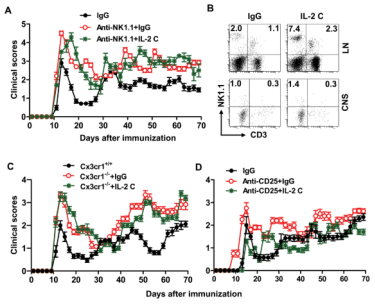

FIGURE 4. Effects of IL-2 complexes on EAE are dependent on CNS-resident NK cells

Groups of mice were immunized with PLP/CFA and treated with IgG or IL-2 complexes (IL-2 C) as indicated in *M&M*. (A) Mice received anti-NK1.1 mAb prior to immunization until termination of the experiment. Clinical features of EAE in these mice were monitored and compared. n=8–12/group. (B) Frequency of NK cells in lymph node and CNS from SJL Cx3cr1$^{-/-}$ mice at days 10–70 p.i. Results are representative of four experiments with 5–12 mice per group each. (C) Clinical features of EAE in SJL Cx3cr1$^{-/-}$ mice that were treated with IgG or IL-2 complexes were monitored and compared. n=10–-12/group. (D) Effects of IL-2 complexes are preserved in PLP/CFA primed mice after CD25^{+} T cell depletion. n = 8/group. P values for clinical scores were evaluated by Mann-Whitney *U* test, other comparisons between groups were analyzed by Student's *t*-test; *p<0.05, **p<0.01.

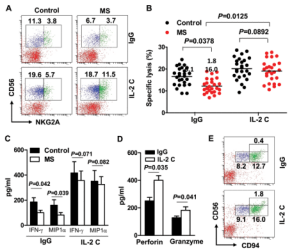

FIGURE 5. IL-2 complexes restore defective NK cells from MS patients

Blood was drawn from relapsing remitting MS patients or healthy controls. Peripheral blood mononuclear cells (PBMC) were isolated and incubated with IgG or a combination of IL-2 (10 ng) and anti-IL-2 mAb (10 μg/ml) for 48–72 hours. (A) Frequency of CD56 and NKG2A double-positive cells on gated $CD3^-$ lymphocytes. Plots are representative of 26 MS patients and 26 controls. Each symbol represents one subject. P values, ANOVA test. (B) $CD56^{dim}$ cells were sorted after incubation with IgG or IL-2 complexes (IL-2 C) and incubated with ^{51}Cr labeled K562 cells. Cytotoxicity toward K562 cells was measured by ^{51}Cr release. (C) $CD56^{bright}$ cells were sorted after incubation with IgG or IL-2 C, production of IFN-γ and MIP-1α was quantified by ELISA. $P<0.01$ for comparisons between different cytokines in the control group and their corresponding IL-2 C treated groups. P values, ANOVA test. (D) Levels of perforin and granzyme B secreted by cultured human NK cells with IgG or IL-2 C were quantified by ELISA. The bar data represents results from two separate experiments (Mean and s.e.m.). P values, Student's *t*-test. (E) Frequency of CD56 and CD94 double-positive cells on gated $CD3^-$lymphocytes. Plots were representative of 6 MS patients.

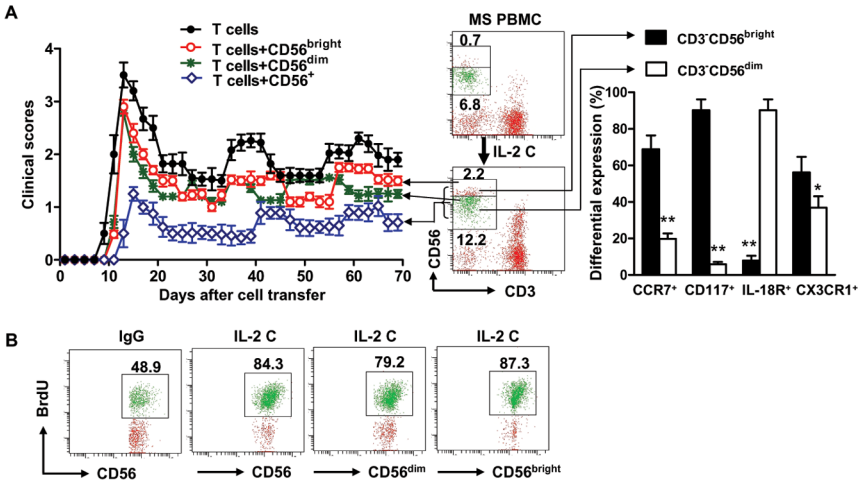

FIGURE 6. Disease protection requires both CD56^{bright} and CD56^{dim} subpopulations

(A) PBMC of control and MS subjects were treated with IL-2 C as described for Fig. 5. CD56^{+}subsets were sorted. CD56^{bright} and CD56^{dim} cells differentially expressed CCR7, CD117, IL-18R and CX3CR1 (right panel). Clinical scores of EAE in RAG1$^{-/-}\gamma c^{-/-}$ mice after co-transferring CD56^{bright} or CD56^{dim} subsets (2.5–5 ×10^{5}) with PLP-reactive T cell lines (1–2 ×10^{6}) raised from the same MS patients whose NK cells are used in the experiments (left panel). P is greater than 0.05 at all time points for comparisons among the group that received T cells only and groups that received T cells together with CD56^{bright} or CD56^{dim} cells. P values varied between 0.036–0.078 at all time points for comparisons among the groups that received T cells together with unfractionated CD56^{+} cells and groups that received T cells together with CD56^{bright} or CD56^{dim} cells. P<0.01 at all time points for comparisons between the groups that received T cells only and groups that received T cells together with unfractioned CD56^{+} cells. P values for clinical scores were evaluated by Mann-Whitney *U* test, n=15–20/group. The expression of differential markers was evaluated by Student's *t*-test, *p<0.05, **p<0.01; n=6 MS subjects. (B) Proliferation of transferred CD56^{+} cells and their subsets was quantified by BrdU. PBMC from 15 donors and 15 recipient animals in each group were studied.

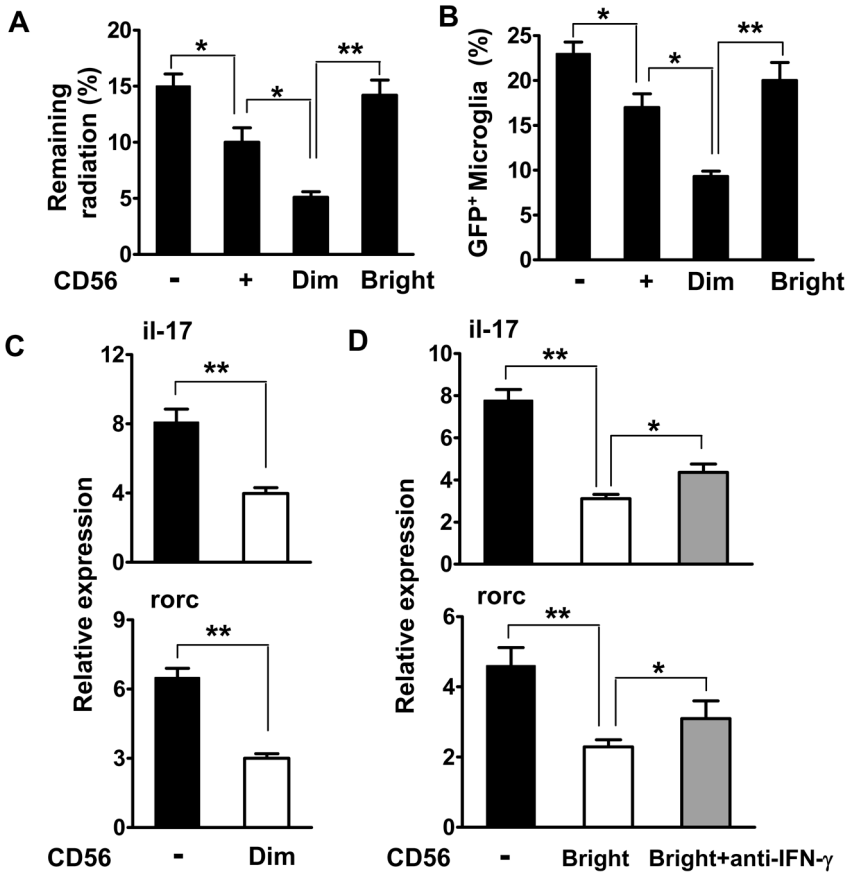

FIGURE 7. Human NK cells employ both cytotoxic and cytokine-mediated mechanisms for disease protection

(A–B) ^{51}Cr labeled-microglia and NK cells were injected into the brain of recipient RAG1$^{-/-}\gamma c^{-/-}$ mice as described in *M&M*. Brains were removed after 8 hours to measure the remaining radioactivity. Efficient killing of microglia by CD56^{dim} NK cells in the brains of mice (A). Percentage of GFP^{+} microglia retention in the brain was measured by FACS (B). (C–D) Human NK cells determine the capacity of microglia to transactivate Th17 cell responses. Isolated naive (CD25^{-}CD62L^{high}CD44^{low}) CD4^{+} T cells were sorted from PBMC. Microglia were sorted from CNS homogenates from Cx3cr1$^{+/-}$ or Cx3cr1$^{-/-}$ mice. NK cells were sorted from PBMC of MS patients and incubated with IL-2 complexes. 2.5–5 $\times 10^{5}$ cells of CD3^{-}CD56^{+}NK cells and the indicated subsets, or microglia were injected into the brain. 1–2 $\times 10^{6}$ PLP-reactive T cells were injected i.v. In some experiments, anti-IFN-γ mAbs (10 μg/ml) were also injected. Rorc and il-17a transcripts were quantified by RT-PCR. Data are representative of three experiments with four mice per group each. All data accumulated from at least three independent experiments. *p<0.05; **p < 0.001 as determined by ANOVA. Human subjects: n=9–12.